

# Indoor Multipath Characterization for MIMO Wireless Communications

Zhongwei Tang and Ananda S. Mohan  
ICT Group, Faculty of Engineering,  
University of Technology, Sydney  
zhongwei@eng.uts.edu.au, ananda@eng.uts.edu.au

## Abstract

*The achievable linear increase in multiple-input multiple-output (MIMO) capacity is conditioned on “sufficiently-rich multipath” presenting in a wireless channel. Thus, the characterization of the resolvable multipaths in an indoor environment dictates the obtainable MIMO capacity at a certain SNR level. In this paper, the statistic relationship between the characteristics of multipaths and the performance of MIMO systems in indoor environments is explored using channel measurements. Our investigations demonstrate the terminology of richness, which is generally used to characterize the multipath propagation, highly relates to the number of effective multipaths, their carried power and their angular features. A novel dimensionless parameter, angular spread factor, is proposed in this work.*

## 1. Introduction

The Multiple-Input Multiple-Output (MIMO) technology is promising to be one of the key techniques for wireless communications beyond 3G, for its high spectrum efficiency and reliability. It is well established that the performance of MIMO systems is dictated by the nature of propagating channels and the resulting fading correlation due to multipath propagation features as well as the antenna mutual coupling. Initial theoretical studies have assumed uncorrelated Rayleigh fading which had led to an ideal MIMO channel matrix with independent and identically distributed (i.i.d.) entries [1, 2]. In realistic scenarios, multipath fading tends to produce correlated channels. The correlation between subchannels will decrease MIMO performance for both indoor and outdoor scenarios. The characteristic of indoor multipath propagation and their impact on the performance of MIMO systems has been of continued interest, particularly for the design and evaluation of MIMO WLAN systems. For this purpose, indoor MIMO channel measurements can offer a straightforward scope for conducting such studies.

A variety of indoor MIMO channel measurements were reported for the investigation of MIMO channel capacity,

spatial correlation etc. Vital for understanding of MIMO channels is the characterization of multipath components existing in a certain communication environment. A “rich-enough scattering environment” is stipulated to allow for an ideal i.i.d. MIMO channel [1, 2]. To achieve a linear increase in MIMO capacity, the channel’s “multipath richness” must exceed the number of antenna elements [3]. Increasing the number of elements beyond the number of multipaths in the channel results in either a low growth-rate or even saturation of the MIMO capacity [4]. Thus it is of practical interest to investigate the resolvable multipaths in an indoor communication environment so as to help to find the mechanisms that affect the achievable MIMO capacity. In this paper, we experimentally investigate the spatial and temporal characterization of multipath propagation in indoor MIMO channels and their inter relationship with the achievable MIMO capacity.

## 2. Indoor MIMO Channel Measurement

The MIMO measurements were performed using a vector network analyzer (VNA) HP 8720A to measure the frequency transfer function at a centre frequency of 2.45 GHz. To obtain a synthetic transmit array, a computer-controlled angular scanner moved a sleeve dipole antenna around a circle to form a virtual four-element uniform circular array (UCA) with a radius of half a wavelength. At the receiver side, a synthetic receive array was obtained using a computer-controlled X-Y scanning system. A synthetic uniform rectangular array was formed by moving a dipole antenna over the horizontal plane. The measurement system was computer-controlled. And for every single transmit and receive antenna pair, 801 frequency response samples were acquired within a bandwidth of 120 MHz. The acquired frequency-response data were saved on a computer via a GPIB interface for post data processing.

Two different measurement environments inside the 28-storey UTS tower building were chosen for the measurement campaign: (i) a classroom (LEC) located on level 23 and (ii) a learning and design centre (LDC1)

room located on level 25, schematically depicted in Figs. 1 and 2. The classroom is a rectangular-shaped lecture room having horizontal dimensions  $14.95 \times 7.46 \text{ m}^2$  and a height of 3.62 m. The room is enclosed by a reinforced concrete wall on one side with a wide metal-framed laminated glass window. The other three sides of the room are enclosed by brick walls, one of which has two wooden door entrances that open into a corridor. There are a number of wooden desks and plastic chairs inside the room. For measurements in LEC, referring to Fig. 1, the transmit antenna was fixed at a position, indicated as B, whilst the receiver was successively located at different positions, indicated as I, D, G, F and H inside the room. During all the measurements, the heights of both the transmit and receive antennas were fixed at 1.7 m above the floor level. We obtained LOS samples in LEC.

LDC1 is a room with large open space and also has an adjoining experimental chamber. The height of this room is 3.62 m. The dimensions of the open area within LDC1 are  $21.20 \times 9.50 \text{ m}^2$ . The building structure of LDC1 is very similar to that of LEC: an external reinforced concrete wall and brick walls separating it from adjacent rooms of this level within the floor and a concrete wall separating it from the stair case. Within the open area of LDC1, a long counter table, 1.50 m above floor level, is located alongside the internal concrete wall. Cubicles, constructed with soft office-partitions with a height of 1.60 m, are located along two side walls, and set with tables with computers. The adjoining experimental chamber, located at one end of LDC1, is a rectangular-shaped room with dimensions of  $5.40 \times 7.40 \text{ m}^2$ . The chamber has a single nest wooden door entrance, and a thin brick wall separates it from the open space of LDC1.

For measurements in LDC1, the transmit antenna was first fixed at a position in the chamber to perform NLOS measurements. In order to acquire LOS channel data, the transmit antenna was later relocated to position LC and the receiver was successively repositioned inside the open area of LDC1. Both the transmit and receive antennas were fixed at a height of 1.7 m above the floor for all measurements.

### 3. Measurement Data Processing

The channel state information is assumed to be known only at the receiver and that equal power allocation scheme is applied at the transmitter. The MIMO channel capacity is calculated as [1]

$$C = \log_2 \det \left( I + \frac{\rho}{n_t} HH^* \right) \quad (1)$$

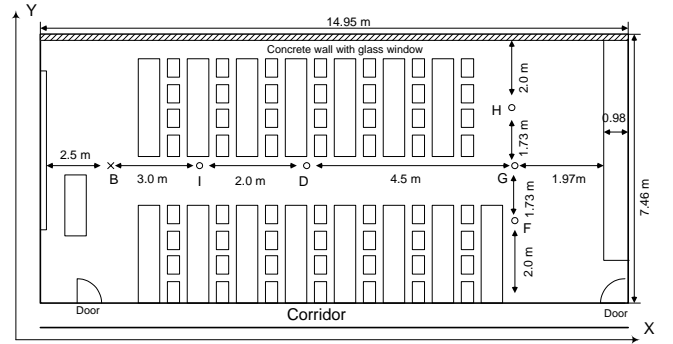


Fig. 1. The deployment of measurements in LEC.

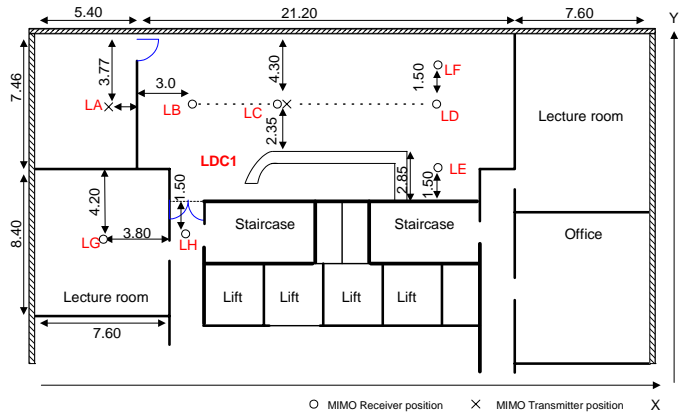


Fig. 2. The deployment of measurements in LDC1.

where  $\det()$  is the matrix determinant,  $n_t$  is the number of transmit antennas,  $\rho$  is the average signal-to-noise ratio (SNR),  $I$  is an identity matrix,  $H^*$  is the Hermitian transpose of  $H$ .

To calculate the measured channel capacity under a certain SNR level, it is necessary that the acquired channel transfer matrices are normalized. We used the Frobenius norm in our calculations, given by

$$\sum_{i=1}^{n_t} \sum_{j=1}^{n_r} |h_{ji}|^2 = n_r n_t \quad (2)$$

where  $h_{ji}$  is the element of the channel transfer matrix,  $n_t$  and  $n_r$  are the number of transmit and receive array elements. When normalized matrices are used in the capacity calculations,  $\rho$  in equation (1) represents the average SNR of a single antenna system. This can be interpreted as the SNR averaged all receive antennas if as signal we consider the power received from all transmit antennas, each one of them transmitting  $P_t/n_t$ . The removal of channel path loss is justified for modelling the subtle effect of spatial correlated propagation.

In this paper, we define the spatial correlation, at the transmit and receive sides, as

$$\rho_{ij,R} = \frac{E(h_{in}h_{jn}^*)}{E(\sqrt{|h_{in}|^2})E(\sqrt{|h_{jn}|^2})} \quad \text{for } n=1 \dots N_T \quad (3)$$

$$\rho_{ij,T} = \frac{E(h_{in}h_{nj}^*)}{E(\sqrt{|h_{ni}|^2})E(\sqrt{|h_{nj}|^2})} \quad \text{for } n=1 \dots N_R \quad (4)$$

where  $h_{in}$  is the measured channel transfer function from the  $n^{\text{th}}$  transmit antenna to the  $i^{\text{th}}$  receive antenna, and similarly for  $h_{jn}$ ,  $h_{ni}$  and  $h_{nj}$ .

The Ricean  $K$  factor, defined as the ratio of the fixed and variable components power, reflects the contribution of the LOS component in LOS channels or the deterministic strongest components in NLOS scenarios to the total channel gain. In our data processing, the  $K$  factor was estimated from measurement data for each MIMO channel using the moment-method [5], averaged over its all corresponding SISO subchannels. The  $K$  factor is estimated as

$$K = \frac{\sqrt{1-\gamma}}{1-\sqrt{1-\gamma}} \quad (5)$$

where  $\gamma = \sigma_r^2 / P_r^2$ ,  $\sigma_r$  is the variance of the received signal power about its mean  $P_r$ .

Further, we have developed a super-resolution algorithm, the Space-Alternating Generalized Expectation-maximization (SAGE), to jointly detect and extract indoor multipath parameters from MIMO measurement data, including the complex amplitude, angle of arrival (AOA) and angle of departure (AOD) [6].

#### 4. Characterization of Indoor MIMO Channels

To investigate this phenomenon, we have extracted multipath parameters, which include the number of multipaths, their path gains, and their angular detail, using the SIC-SAGE algorithm. A cutoff threshold of 30 dB below the strongest path was set as a condition of convergence in the SIC-SAGE algorithm.

Fig.3 shows the complementary cumulative distribution function (CCDF) of the number of effective multipath components for LOS and NLOS indoor channels. Overall, the results indicate that more multipaths are encountered for NLOS indoor scenarios than that for LOS indoor scenarios. In our measurements, less than 35% of the total LOS channels have more than 30 MPCs; whereas 82% of the NLOS scenarios have more than 30 MPCs. As far as the capacity improvement offered by rich multipath is concerned, the results on

MIMO capacity as a function of the number of multipath components are shown in Fig.4 for the two indoor scenarios considered. The measured 4x4 MIMO capacity is calculated using (1) with SNR equal to 20 dB. The 4x4 MIMO link was established between a 4-element transmit UCA and a 4-element square receive array. As can be seen, the MIMO capacity increases with increasing number of effective multipaths. However, there appears an increasing trend for LOS scenarios having a steeper curve than that for NLOS scenarios. The increase in multipaths in LOS channels will degrade the Ricean  $K$  factor, thereby increasing the capacity.

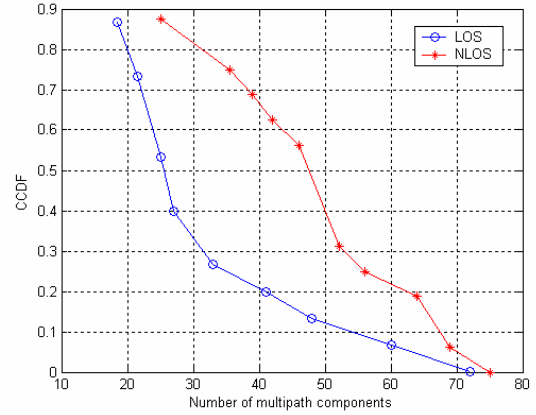


Fig.3. Number of effective MPCs.

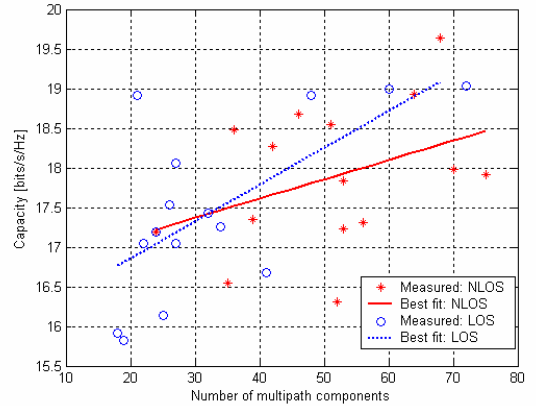


Fig.4. Capacity versus the number of effective MPCs.

A widely-used measure for the angular variation of multipath components in the literature is the angle spread [7]. However, in our results, this parameter does not show expected correlation with the obtained MIMO capacity. The reason can be explained as: theoretically, the effect on the spatial correlation between two adjacent antennas due to a multipath with an AOA of  $2^\circ$  is the same as that

due to one with an AOA of  $182^\circ$  if they carry the same power; however their impact on the angle spread is obviously different in the widely-used term. Thus we feel it is necessary to define an appropriate variable to represent the angular feature of multipath propagation for a MIMO channel. It is well known that the spatial correlation between two adjacent identical antennas due to the arrival of a single plane wave can be approximated as a function of its incident angle,  $\phi$ , as

$$\rho(d) = e^{-j\frac{2\pi d}{\lambda}\cos\phi} \quad (6)$$

where  $d$  is the antenna separation. Now we define a new dimensionless parameter “angle spread factor (ASF),  $\sigma_\phi$ ” to describe the effect of the angular properties of multipath components on MIMO performance, at each end of a MIMO link, given by

$$\sigma_\phi = \sqrt{\frac{\sum_{l=1}^L |\alpha_l|^2 |\cos\phi_l|^2}{\sum_{l=1}^L |\alpha_l|^2} - \left(\frac{\sum_{l=1}^L |\alpha_l|^2 |\cos\phi_l|}{\sum_{l=1}^L |\alpha_l|^2}\right)^2} \quad (7)$$

For each MIMO link, we have two angle spread factors,  $\sigma_{\phi,T}$  at the transmitter and  $\sigma_{\phi,R}$  at the receiver, respectively. The ASF is a measure of the effect of angular variations of multipath components as well as their carried power on the spatial correlation between array elements. Due to the double directional nature of a MIMO channel, it is important to consider the individual parameters at both ends of the MIMO link.

The results on spatial correlation as a function of the angle spread factor at the receiver side are plotted in Fig.5 for indoor NLOS channels. As expected, a smaller angular spread factor results in a higher spatial correlation. The same trend was also observed for LOS indoor channels. Fig.6 plots the capacity versus the angle spread factor for both LOS and NLOS indoor channels. The value of angle spread factor, shown in the figure, is the sum of the two angle spread factors at both ends of a MIMO link. As can be seen, the MIMO capacity increases with increasing angle spread factor for both LOS and NLOS scenarios. The best fit line demonstrates that the effect of the angle spread factor on LOS MIMO capacity is sharper than on NLOS MIMO capacity. Thus it is clear that both the number of multipaths and their angular features affect the MIMO performance.

Fig.7 presents the number of extracted multipath components as a function of the Ricean  $K$  factor. The measurement data demonstrate that the number of effective multipaths decreases with increasing values of Ricean  $K$  factor. The results reveal that, the higher the value of Ricean  $K$  factor, the greater the contribution of

the LOS component, which reduces the detectable multipaths. Consequently, MIMO capacity for such a channel is also degraded.

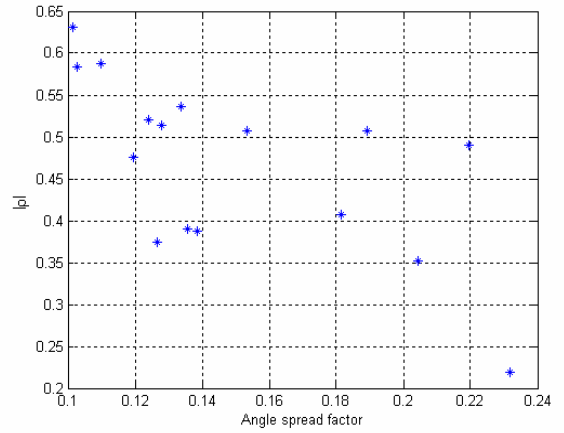


Fig.5. Spatial correlation as a function of ASF for NLOS scenarios.

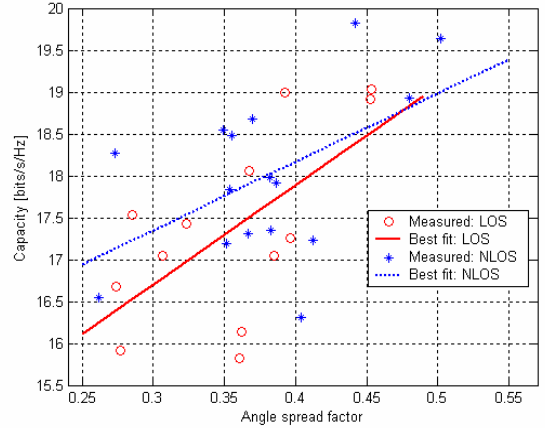


Fig.6. Capacity versus ASF.

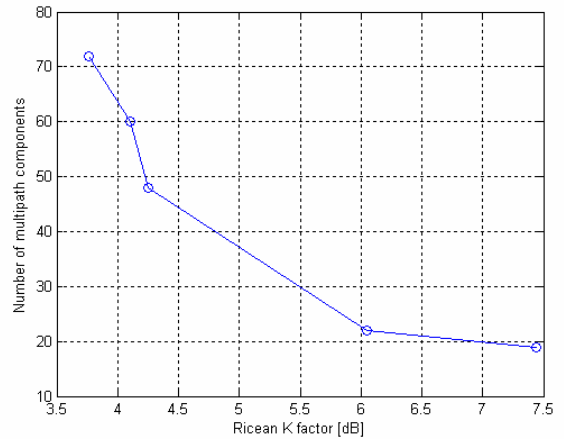


Fig.7. The number of multipaths versus Ricean  $K$  factor.

## 5. Conclusions

This paper has explored the statistical characterization of multipath propagation in indoor environments by employing the super-resolution SAGE algorithm on measurement data. The characteristics of indoor multipath propagation and its effect on MIMO capacity have been investigated for both LOS and NLOS scenarios. A novel parameter, angle spread factor is proposed to characterize the close relationship between the multipath angular spread feature and MIMO performance. Our results reveal that the achievable indoor MIMO capacity is a function of the dominant propagation mechanisms, such as the number of effective multipaths, their angular features and the carried power.

## 6. Acknowledgement

The project is funded by the Australian Research Council through an industry linkage grant program with Singtel Optus Pty Ltd.

## 7. References

- [1] G. J. Foschini and M. J. Gans, "On limits of wireless communications in a fading environment," *Wireless Personal Communications*, vol. 6, pp. 311-335, Mar.1998.
- [2] I. E. Telatar, "Capacity of multi-antenna gaussian channels," *European Trans. Telecomm.*, vol. 10, pp. 585-595, Nov. 1999.
- [3] J. P. Kermoal, L. Schumacher, K. I. Pedersen, P. E. Mogensen, and F. Frederiksen, "A stochastic MIMO radio channel model with experimental validation," *IEEE J. Select. Areas Commun.*, vol. 20, pp. 1211 -1226, Aug. 2002.
- [4] G. G. Raleigh and J. M. Cioffi, "Spatio-temporal coding for wireless communication," *IEEE Trans. Commun.*, vol. 46, pp. 357 - 366, March 1998.
- [5] L. J. Greenstein, D. G. Michelson, and V. Erceg, "Moment-method estimation of the Ricean K-factor," *IEEE Commun. Lett.*, vol. 3, pp. 175-176, June 1999.
- [6] B. H. Fleury, P. Jourdan, and A. Stucki, "High-resolution channel parameter estimation for MIMO applications using the SAGE algorithm," in proc. 2002 International Zurich Seminar on Broadband Communications, Access, Transmission, Networking, 2002, pp. 30-1 -30-9.
- [7] R. Vaughan and J. B. Andersen, *Channels, Propagation and Antennas for Mobile Communications*. London: The Institution of Electrical Engineers, 2003.